8494 *Biochemistry* **2009,** *48,* 8494–8504
DOI: 10.1021/bi900578y

BIOCHEMISTRY
including biophysical chemistry & molecular biology
Article

Fluconazole Modulates Membrane Rigidity, Heterogeneity, and Water Penetration into the Plasma Membrane in *Saccharomyces cerevisiae*[†]

Fumiyoshi Abe,* Keiko Usui, and Toshiki Hiraki

Molecular Evolution and Adaptation Research, Institute of Biogeosciences, Japan Agency for Marine-Earth Science and Technology (JAMSTEC), Yokosuka 237-0061, Japan

Received April 5, 2009; Revised Manuscript Received July 14, 2009

ABSTRACT: Azole anitifungal drugs such as fluconazole inhibit 14α-demethylase. The mechanism of fluconazole action on the plasma membrane is assumed to be ergosterol depletion and accumulation of a toxic sterol, 14α-methyl-3,6-diol, that differs in C-6 hydroxylation, B-ring saturation, C-14 methylation, and side-chain modification. Nevertheless, little is known about how these sterol modifications mechanically influence membrane properties and hence fungal viability. Employing time-resolved measurement with a fluorescence anisotropy probe, 1-[4-(trimethylamino)phenyl]-6-phenyl-1,3,5-hexatriene (TMA-DPH), we demonstrated that fluconazole administration decreased the rigidity of the plasma membrane of *Saccharomyces cerevisiae*, leading to a dramatic reduction in the order parameter (*S*) from 0.965 to 0.907 and a 5-fold acceleration of the rotational lipid motion. This suggests that the altered sterol has a deleterious impact on membrane packing, resulting in increased fluidity. Deletion of *ERG3* confers hyperresistance to fluconazole by circumventing the accumulation of 14α-methyl-3,6-diol and instead produces 14α-methylfecosterol lacking the 6-OH group. We found that *ERG3* deletion mitigated the fluconazole-induced loss of membrane rigidity with *S* remaining at a higher value (= 0.922), which could contribute to the fluconazole resistance in the *erg3*Δ mutant. The reduced ability of the 6-OH sterol to stiffen lipid bilayers was supported by the finding that 30 mol % of 6α-hydroxy-5α-cholestanol marginally increased the *S* value of 1-palmitoyl-2-oleoyl-*sn*-glycero-3-phosphocholine membranes, while cholesterol and dihydrocholesterol markedly increased it. The decay of the TMA-DPH fluorescence was bimodal in the wild-type strain. This heterogeneity could have arisen from varying degrees of water penetration into the plasma membrane. Fluconazole eliminated the heterogeneity of the dielectric characteristic of the membrane interfacial region, and concomitantly the TMA-DPH lifetime was shortened. Therefore, we conclude that 14α-methyl-3,6-diol is insufficient to pack the plasma membrane, allowing water penetration, which is consistent with membrane disorder after fluconazole administration. Our findings illustrate the role of ergosterol in maintaining membrane heterogeneity and preventing water penetration as well as maintaining the rigidity of the plasma membrane interfacial region.

Fungal infections have become a considerable problem in recent years, especially in immunocompromised patients (*1*, *2*). Azoles are major drugs used to treat pathogenic infection by yeasts such as *Candida albicans* and *Candida glabrata*. Fluconazole is an excellent triazole antifungal agent that selectively inhibits the sterol C-14α-demethylase encoded by the *ERG11* gene (*3*), but the resistance of *Candida* species to azoles is reported with increasing frequency. Several mechanisms are proposed to account for resistance to azoles: (i) reduction in intracellular accumulation of azoles by enhanced drug efflux pumps,; (ii) increased levels of the azole cellular target, and (iii) alterations in sterol synthesis by deletion of the *ERG3* gene (*4*, *5*). *Saccharomyces cerevisiae* has been used to elucidate the molecular mechanisms of fluconazole resistance. The mechanism by which fluconazole inactivates yeasts is presumed to be the depletion of ergosterol and the accumulation of toxic sterols, especially 14α-methyl-3,6-diol (*6*, *7*). 14α-Methyl-3,6-diol is structurally different from ergosterol in terms of the absence of B-ring unsaturation, the presence of the 6-OH group and the additional C-14 methyl group, and side-chain modification. In particular, the polar 6-OH group of this altered sterol is thought to interfere with sterol−phospholipid packing in the plasma membrane, causing membrane damage and growth inhibition. However, little is known about how the altered sterol mechanically influences the properties of the plasma membrane *in vivo*, such as packing efficiency, rigidity, and permeability. It is known that deletion of the *ERG3* gene that encodes Δ5,6-desaturase confers fluconazole resistance by circumventing the accumulation of 14α-methyl-3,6-diol and instead producing 14α-methylfecosterol, a less toxic sterol (*6*). Despite the clear structural difference, it is still unexplained how each altered sterol affects the mechanistic properties of the plasma membrane and determines physiologic traits. It is necessary to elucidate the fluconazole-induced changes in the membrane to increase our knowledge of azole resistance and develop better chemotherapeutic regimens for the treatment of fungal infections. Comparison of the membrane properties between the wild-type strain and *erg3*Δ mutant with or without fluconazole administration can reveal the requirement for the structural motifs of sterol to explain fluconazole toxicity in terms of C-6 hydroxylation, B-ring saturation, C-14 methylation, and side-chain modification.

Fluorescence depolarization techniques are highly sensitive to probe the dynamic properties of both artificial lipid bilayers and natural cell membranes in terms of membrane order and the

[†]This work was supported by the Japan Society for the Promotion of Science (No. 18658039 to F.A.).
*Corresponding author. Tel: +81-46-867-9678. Fax: +81-46-867-9715. E-mail: abef@jamstec.go.jp.

 Published on Web 08/11/2009

rotational motion of lipid acyl chains. Two lipophilic molecules, 1,6-diphenyl-1,3,5-hexatriene (DPH) and 1-[4-(trimethylamino)-phenyl]-6-phenyl-1,3,5-hexatriene (TMA-DPH),[1] are commonly utilized in such experiments (*8*−*10*). DPH primarily distributes perpendicular to the bilayer plane near the center of the membrane but partially distributes parallel to it within the acyl chain tails (*11*). TMA-DPH, a cationic derivative of DPH, is anchored with the charged headgroup at the lipid−water interface and thereby reflects only the interfacial region of the membrane. Mutants of *S. cerevisiae* defective in the final five steps of ergosterol biosynthesis are viable but accumulate structurally altered sterols within the plasma membrane. Parks and colleagues reported that membrane rigidity is lost in sterol auxotrophs (*12*). The changes in sterol composition caused by *erg* mutations confer pleiotropic hypersensitivity to a broad range of chemicals such as ethanol, cycloheximide, anthracyclines, dactinomycin, and brefeldin A (*13*−*15*). Prasad and colleagues reported that the changes in membrane fluidity and increased drug diffusion alone might not be sufficient to result in the observed hypersensitivities of the *erg* mutants but that the alterations in the sterol−lipid interactions could be more relevant to drug hypersensitivity (*16*). We used time-resolved anisotropy measurement of TMA-DPH-labeled cells based on time-correlated single-photon counting (TCSPC) to describe the phenotypic abnormalities of five *erg* mutants consistent with changes in dynamic membrane properties represented by the order parameter and rotational lipid motion (*17*). Specifically, deletion of *ERG2* results in the greatest decrease in the membrane order parameter and increase in rotational lipid motion, providing evidence that voids occur within the *erg2*Δ plasma membrane and that specific structural motifs of ergosterol have a role in packing the lipid bilayer. The decreasing membrane order and increasing occurrence of voids synergistically enhance passive diffusion of cycloheximide across the membrane, accounting for the cycloheximide sensitivity of the *erg* mutants (*17*). In our genome-wide functional screening, we found that the growth of the *erg* mutants was hypersensitive to high hydrostatic pressure of 25 MPa (approximately 250 kg/cm^2) and low temperature of 15 °C (*18*). This suggests that ergosterol but not altered sterols mitigates the adverse influences of high pressure and low temperature that pack the bilayer membrane and restrict the acyl chain motion. The possibility of characterizing membranes using the optical technique could improve our knowledge of membrane structure and membrane-associated events such as drug permeability, vesicle fusion, and membrane protein function.

This study provides mechanistic evidence that fluconazole administration decreases the membrane rigidity associated with modifications of sterol structure and enhances water penetration by eliminating the heterogeneity of the dielectric characteristic of the plasma membrane. Comparing the membrane between the wild-type strain and the *erg3*Δ mutant, we correlate individual modifications in sterol structure with changes in membrane properties *in vivo* and with drug toxicity.

EXPERIMENTAL PROCEDURES

Yeast Strains and Culture Conditions. The wild-type *S. cerevisiae* strain BY4742 (*MAT*α *his3*Δ*1 leu2*Δ*0 lys2*Δ*0 ura3*Δ*0*) and the *erg3*Δ::*kanMX4* mutant were obtained from the EUROSCARF yeast-deletion library (catalog no. 95400.H3; Invitrogen, Carlsbad, CA) (*19*). Cells were grown in synthetic complete (SC) medium with slight modification (*20*) with vigorous shaking at 25 °C. The optical density at 600 nm (OD_{600}) was measured after appropriate dilution of the samples. Fluconazole (Wako Pure Chemical Industries Inc., Osaka, Japan) was dissolved in SC medium or ethanol to give a stock solution of 20 or 100 mM, respectively. TMA-DPH (Invitrogen) was dissolved in DMSO to give stock solutions of 5 mM.

Determination of the IC_{50} Value of Fluconazole. To determine the 50% growth inhibitory concentration (IC_{50}) of fluconazole, exponentially growing cells were diluted in SC medium at 0.001 OD_{600} (10^4 cells·mL^{-1}), and the cells were exposed to various concentrations of the drug in 96-well plates at 25 °C. After 48 h, the OD_{600} was measured using an MTP-450 plate reader (Corona Electric Co., Ltd., Hitachinaka, Japan). Data are expressed as mean OD_{600} values with standard deviations from three independent experiments.

Labeling of Cells with TMA-DPH. Cells were labeled with TMA-DPH as described previously (*17*). Briefly, exponentially growing cells at 0.5−1.0 OD_{600} (0.5−1.0 × 10^7 cells·mL^{-1}) were washed twice with TE buffer (10 mM Tris-HCl, 1 mM EDTA, pH 7.0) and labeled with 0.5 μM TMA-DPH at 25 °C for 10 min in the dark. After washing twice, the cells were resuspended in TE buffer at 0.2 OD_{600} and subjected to time-resolved fluorescence anisotropy measurement.

Isolation of the Plasma Membrane and Labeling. The plasma membrane was purified from cells as described previously with some modifications (*20*). Cells (0.2 OD_{600}) were cultured in SC medium with or without 100 μM fluconazole for 12 h. Then, 10^9 cells were collected by centrifugation, washed twice in TE buffer, and broken with glass beads. An equal volume of 2-morpholinoethanesulfonic acid (MES) buffer (50 mM MES, 1 mM $MgCl_2$, pH 5.2) was added to the lysate to lower the pH. The lysate was centrifuged at 1000*g* for 5 min and 3000*g* for 5 min to remove unbroken cells and mitochondria. The resulting supernatant was centrifuged at 13000*g* for 10 min to obtain the P13 membrane pellet. To isolate the plasma membrane, the P13 membrane was placed on a stepwise gradient of 20%, 40%, and 50% sucrose and centrifuged at 100000*g* for 18 h at 4 °C using a TLS55 rotor (Beckman Instruments Inc., Fullerton, CA) (*20*). The resulting purified plasma membrane pellet was dissolved in 100 μL of TE buffer followed by labeling with 0.5 μM TMA-DPH. After 10 min, 2 mL of TE buffer was added to dilute the labeling mixture. Because TMA-DPH is nonfluorescent in aqueous solution, the background fluorescence of the mixture was negligible.

Preparation of POPC Membrane Vesicles. 1-Palmitoyl-2-oleoyl-*sn*-glycero-3-phosphocholine (POPC; Wako Pure Chemical Industries Inc.), cholesterol (Wako Pure Chemical Industries Inc.), dihydrocholesterol (β-cholestanol; Sigma-Aldrich, Inc., St. Louis, MO), 6α-hydroxy-5α-cholestanol (Avanti Polar Lipids, Inc., Alabaster, AL), and TMA-DPH were dissolved in chloroform. POPC was mixed with 30 mol % of cholesterol, dihydrocholesterol, or 6-hydroxy-5α-cholestanol and 0.01 mol % of TMA-DPH, and the solvent was removed under a vacuum. It was suspended in TE buffer with a vortex and sonication. The membranes were allowed to swell in TE buffer at 25 °C for 1 h, and the OD_{600} value was adjusted to 0.2 prior to anisotropy measurement.

Time-Resolved Fluorescence Spectroscopy. Measurement of time-resolved fluorescence anisotropy was performed as

[1]Abbreviations: TMA-DPH, 1-[4-(trimethylamino)phenyl]-6-phenyl-1,3,5-hexatriene; POPC, 1-palmitoyl-2-oleoyl-*sn*-glycero-3-phosphocholine; TCSPC, time-correlated single-photon counting; r_0, maximum anisotropy; r, limiting anisotropy; θ, rotational correlation time; S, order parameter; D_w, rotational diffusion coefficient; τ, fluorescence lifetime.

described previously (*17*). Briefly, a FluoroCube (Horiba Ltd., Kyoto, Japan) capable of performing TCSPC was used with a polarizing device and a 375 nm laser diode (NanoLED 375 L; Horiba Ltd.). TMA-DPH-labeled cells were placed in a quartz cuvette at 0.2 OD_{600}. Fluorescence was emitted at 460 nm at 25 °C. The simplest model of the restricted motion of fluorochromes in the membrane, based on the Brownian diffusion of the label in a cone with a wobbling diffusion constant, leads to the following single-exponential approximation of the anisotropy decay with time, $r(t)$ (*8*):

$$r(t) = (r_0 - r_\infty)\exp(-t/\theta) + r_\infty \quad (1)$$

where r_0 stands for the maximum anisotropy, r_∞ for limiting anisotropy, and θ (ns) for rotational correlation time. The order parameter (S) is calculated to obtain structural information on the membrane according to the equation:

$$S = (r_\infty/r_0)^{1/2} \quad (2)$$

The rotational (wobbling) diffusion coefficient (D_w) was calculated to obtain the dynamic nature of the membrane according to the equation:

$$D_w = (r_0 - r_\infty)/6\theta r_0 \quad (3)$$

An approximation of the fluorescence decay with time, $I(t)$, is described by the following equation containing three exponential discrete decay components:

$$I(t) = A_1\exp(-t/\tau_1) + A_2\exp(-t/\tau_2) + A_3\exp(-t/\tau_3) \quad (4)$$

where τ is the fluorescence lifetime and A the amplitude of each fraction. For most experiments in this study, the goodness of fit, as expressed by χ^2, was improved by the use of a triexponential rather than biexponential or monoexponential fluorescence decay function. A multiexponential function is commonly used in decay analysis in artificial lipid bilayer systems (*21*−*23*).

Fluorescence Microscopy. An FV500 confocal laser microscope equipped with a 405 nm UV laser (Olympus Corporation, Tokyo, Japan) was used to visualize TMA-DPH-labeled cells (*17*). The proportion of abnormally labeled cells was calculated by counting 170−300 cells on fluorescence images.

RESULTS

Deletion of ERG3 Confers Fluconazole Resistance. Figure 1 illustrates the structures of ergosterol and altered sterols that accumulated in the plasma membrane when the wild-type and *erg3*Δ cells of *S. cerevisiae* were exposed to fluconazole. We first examined whether fluconazole resistance had been conferred on the *erg3*Δ mutant isogenic to strain BY4742. The IC_{50} values of fluconazole were determined by measuring OD_{600} at 48 h in static cultures after the cells had been exposed to various concentrations of fluconazole. Consistent with reports in the literature (*6*, *7*), deletion of *ERG3* conferred a dramatic resistance to fluconazole of greater than 100-fold compared with the wild-type cells, and the IC_{50} value changed from 36.3 ± 2.8 μM (= 11.1 ± 0.9 μg/mL; wild type) to 4.2 ± 0.4 mM (= 1.3 ± 0.1 mg/mL; *erg3*Δ) (Figure 2A). Figure 2B illustrates the time course of growth in shaking culture after the addition of fluconazole. Cells of both the wild-type and *erg3*Δ strains normally proliferated for the initial 6 h, corresponding to three cell divisions. This is nearly consistent with a previous report that

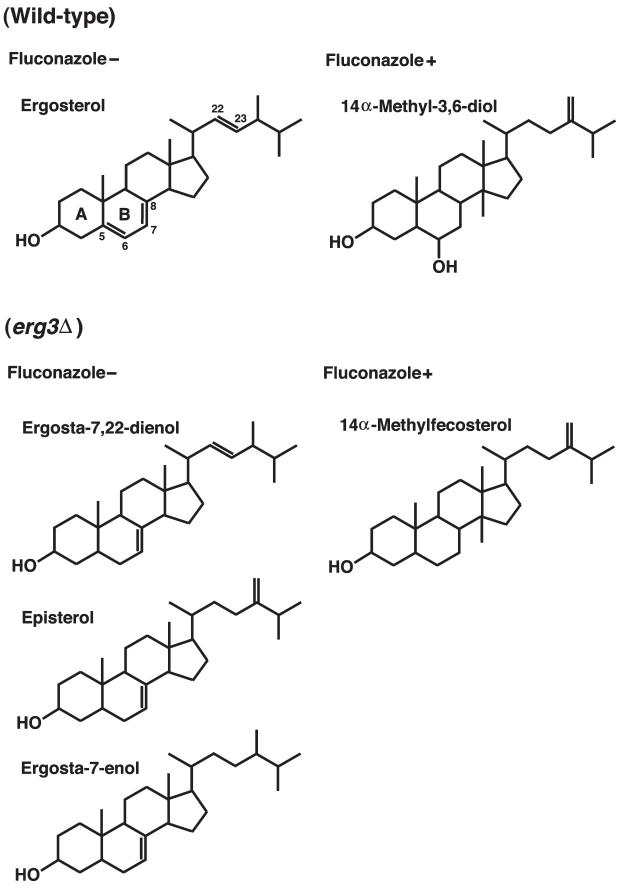

FIGURE 1: Structures of ergosterol and altered sterols accumulated in cells of (A) the wild-type strain and (B) the *erg3*Δ mutant with (right) or without (left) fluconazole treatment. The structures of altered sterols were reported in refs *7* and *30*.

cells undergo seven to nine doublings on a YPD plate after fluconazole addition (*24*). Whereas *erg3*Δ cells continued to grow after 6 h, wild-type cells no longer proliferated in the presence of 100 μM fluconazole. Hyperresistance of the *erg3*Δ mutant to fluconazole is thought to occur by circumventing the accumulation of the toxic sterol 14α-methyl-3,6-diol and instead allowing the accumulation of nontoxic 14α-methylfecosterol (*6*, *7*). We speculate that the effects of fluconazole administration on the accumulation of these sterols differentially alter the properties of the plasma membrane.

Fluconazole Treatment Decreases the Rigidity of the Plasma Membrane in Intact Cells. To investigate the effects of fluconazole on membrane properties, we characterized the rotational motion of TMA-DPH embedded in the plasma membrane. Cells were cultured in SC medium containing 100 μM fluconazole, a concentration 3-fold higher than the IC_{50} for the wild-type strain and 40-fold lower than the IC_{50} for the *erg3*Δ mutant. After labeling with TMA-DPH, the cells were analyzed using time-resolved fluorescence anisotropy measurement. Figure 3A shows typical anisotropic decay of TMA-DPH in intact cells. As reported previously (*17*), the limiting anisotropy (r_∞) value of TMA-DPH remained high at around 0.3 in both strains, confirming the marked rigidity of the interfacial region of the yeast plasma membrane in contrast to artificial lipid bilayers in the liquid crystalline phase. Strikingly, fluconazole treatment caused a significant decrease in r_∞ to around 0.26, suggesting that the plasma membrane becomes markedly disordered (Figure 3A). The nonlinear fitting of the decay after convoluting

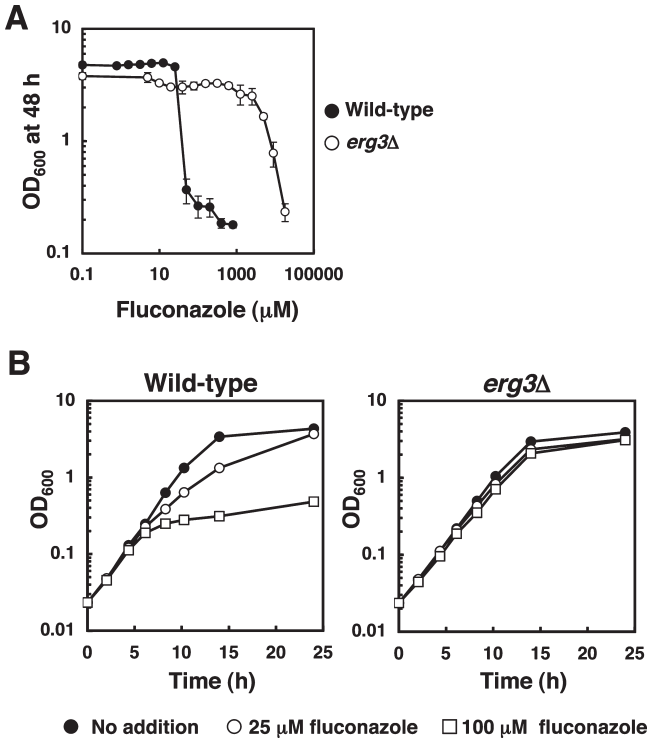

FIGURE 2: Fluconazole sensitivity of the wild-type strain and *erg3*Δ mutant. (A) Cells with an OD_{600} value of 0.001 were cultured in SC medium in the presence of various concentrations of fluconazole for 48 h. Data are expressed as mean OD_{600} values with standard deviations from three independent experiments. (B) Growth profile of the wild-type and *erg3*Δ strains after the addition of 25 or 100 μM fluconazole to the cultures at 0.02 OD_{600}. The wild-type cells showed growth arrest at 6 h, while the *erg3*Δ cells continued to grow. Typical data from three independent experiments are shown.

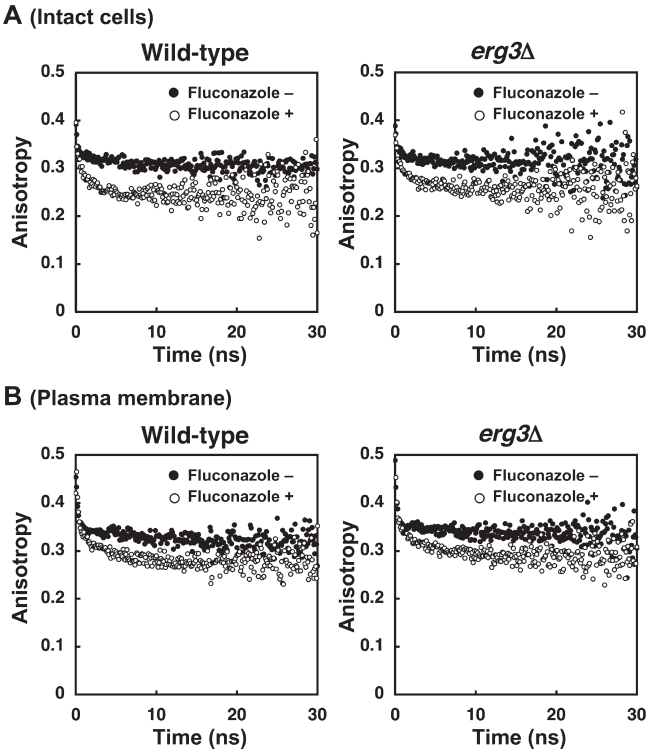

FIGURE 3: Time-resolved anisotropy measurement of TMA-DPH in intact cells and the plasma membrane isolates. Cells of the wild-type strain and the *erg3*Δ mutant were cultured in the presence or absence of 100 μM fluconazole for 12 h. The cells (A) or the plasma membrane isolated (B) was labeled with 0.5 μM TMA-DPH and subjected to time-resolved anisotropy measurement. The parameters characterizing anisotropy decay are presented in Tables 1 and 2.

the instrumental response function gave parameters describing the rotational motion of TMA-DPH and hence the rotational lipid motion in the interfacial region where sterol molecules were enriched. In the wild-type cells, the order parameter S was 0.956 ± 0.006 ($n = 10$), and it remained almost unchanged 2 h after the addition of fluconazole to the cell cultures (Table 1). It started to decrease at 4 h, and it reached 0.864−0.899 at 6−12 h after the addition of fluconazole to the culture. The rotational diffusion coefficient D_w was $1.3 \pm 0.6\ \mu s^{-1}$ ($n = 10$) before the addition of fluconazole. Concomitant with the decrease in S, D_w started to increase 4 h after fluconazole addition and reached around $20\ \mu s^{-1}$ at 6−12 h (Table 1). This indicates that the rotational motion of TMA-DPH was markedly accelerated. Therefore, we speculate that the substitution of 14α-methyl-3,6-diol for ergosterol decreased membrane rigidity and thereby gave rise to voids within the plasma membrane. It should be noted that the fluconazole-induced changes in S and D_w were more marked than those seen after any single deletion of *ERG2*, *ERG3*, *ERG4*, *ERG5*, and *ERG6* in the absence of fluconazole treatment (*17*). Fluconazole exerted similar effects on the *erg3*Δ plasma membrane, but they were moderate compared with those in the wild-type cells. We found that S remained higher (0.893−0.917) and D_w remained lower ($14.0-17.4\ \mu s^{-1}$) in the *erg3*Δ cells than in the wild-type cells (S, 0.864−0.899, and D_w, $19.6-21.2\ \mu s^{-1}$) more than 6 h after fluconazole treatment (Table 1). These results suggest that 14α-methyl-3,6-diol has less ability to stiffen the lipid bilayer than 14α-methylfecosterol. The relevance of membrane rigidity in fluconazole resistance is discussed below. We found that the accumulation of rhodamine 6G increased with time after the addition of 100 μM fluconazole to the culture in both the wild-type and *erg3*Δ cells (data not shown), suggesting that the loss of membrane rigidity and concomitant spacing between the lipid headgroups enhance passive diffusion of the dye across the plasma membrane.

In the course of this study, we noted that fluconazole treatment caused TMA-DPH to mislocalize in 16−29% of the cell population. In those cells, TMA-DPH was distributed throughout the cytoplasm after fluconazole treatment (Figure 4, arrowheads). This could lead to an incorrect assessment of plasma membrane properties incorporating anisotropy decay from the cytoplasmic TMA-DPH. To avoid this, we next elucidated the properties of the isolated plasma membrane.

Measurement of Fluorescence Anisotropy of Isolated Plasma Membranes. The plasma membranes were isolated from cells that had been cultured in SC medium for 12 h in the presence of 100 μM, or 10 mM fluconazole, which is an inhibitory concentration for growth of the *erg3*Δ mutant (Figure 2A). The relative purity of the plasma membrane isolates was estimated by quantifying certain membrane marker proteins in Western blotting (*20*). The incorporation of Pma1 (the plasma membrane), Pep12 (endosomal membrane), and Vps10 and ALP (vacuolar membrane) in the plasma membrane pellet was >99%, 1.2%, 0.3%, and 1.5%, respectively, which was sufficiently pure to verify the plasma membrane properties. The membrane isolates were labeled with TMA-DPH and analyzed using time-resolved fluorescence anisotropy measurement. There was no marked difference in S and D_w between intact cells and the corresponding isolated plasma membrane (Tables 1 and 2). In agreement with the results in intact cells, 100 μM fluconazole treatment exerted a

Table 1: Effects of Fluconazole on the Anisotropy Decay of TMA-DPH in the Wild-Type and *erg3*Δ Cells[a]

time after FLC addition (h)	θ (ns)	r_0	r_∞	S^b	D_w (μs^{-1})^b	$S/D_w{}^b$	χ^2	n
				Wild-Type Cells				
0	11.5 ± 2.6	0.335 ± 0.009	0.306 ± 0.011	0.956 ± 0.006	1.3 ± 0.6	0.78 ± 0.17	1.09 ± 0.04	10
2	10.6 ± 4.6	0.339 ± 0.004	0.312 ± 0.004	0.959 ± 0.004	1.5 ± 0.8	0.78 ± 0.39	1.14 ± 0.04	5
4	1.8 ± 0.5	0.340 ± 0.008	0.292 ± 0.007	0.928 ± 0.01**	14.6 ± 6.0**	0.07 ± 0.03**	1.06 ± 0.01	6
6	1.9 ± 0.1	0.336 ± 0.007	0.255 ± 0.002	0.870 ± 0.007**	21.2 ± 1.4**	0.04 ± 0.003**	1.06 ± 0.09	4
8	2.1 ± 0.2	0.334 ± 0.003	0.249 ± 0.002	0.864 ± 0.006**	20.8 ± 2.5**	0.04 ± 0.006**	1.04 ± 0.03	4
10	1.9 ± 0.3	0.339 ± 0.003	0.263 ± 0.007	0.881 ± 0.008**	19.6 ± 4.0**	0.05 ± 0.01**	1.07 ± 0.05	4
12	1.7 ± 0.4	0.334 ± 0.019	0.270 ± 0.022	0.899 ± 0.016**	20.8 ± 7.1**	0.05 ± 0.02**	1.11 ± 0.06	11
				*erg3*Δ Cells				
0	3.3 ± 1.5	0.346 ± 0.008	0.323 ± 0.009	0.966 ± 0.008	4.0 ± 2.2	0.29 ± 0.13	1.05 ± 0.03	8
2	2.2 ± 1.7	0.345 ± 0.007	0.316 ± 0.013	0.957 ± 0.015	9.7 ± 6.7*	0.18 ± 0.18	1.09 ± 0.06	6
4	2.6 ± 1.2	0.346 ± 0.013	0.314 ± 0.010	0.952 ± 0.008*	7.8 ± 5.3	0.17 ± 0.11	1.10 ± 0.07	6
6	1.9 ± 0.4	0.340 ± 0.006	0.280 ± 0.005	0.907 ± 0.007**	16.4 ± 3.0**	0.06 ± 0.01*	1.04 ± 0.04	4
8	1.8 ± 0.1	0.340 ± 0.003	0.277 ± 0.006	0.903 ± 0.008**	16.7 ± 2.1**	0.06 ± 0.008*	1.14 ± 0.06	4
10	2.0 ± 0.5	0.343 ± 0.009	0.289 ± 0.014	0.917 ± 0.012**	14.0 ± 4.5**	0.07 ± 0.02*	1.06 ± 0.02	4
12	2.0 ± 0.4	0.333 ± 0.017	0.266 ± 0.019	0.893 ± 0.019**	17.4 ± 4.1**	0.06 ± 0.02**	1.10 ± 0.07	11

[a]Cells were incubated in the presence of 100 μM fluconazole. Measurements were carried out at 25 °C. Data are represented as mean ± SD. Key: FLC, fluconazole; θ, rotational correlation time; r_0, maximum anisotropy; r_∞, limiting anisotropy; S, order parameter; D_w, rotational diffusion coefficient; n, number of independent experiments. [b]Asterisks denote statistical significance with respect to no fluconazole treatment (*, $P < 0.05$; **, $P < 0.005$).

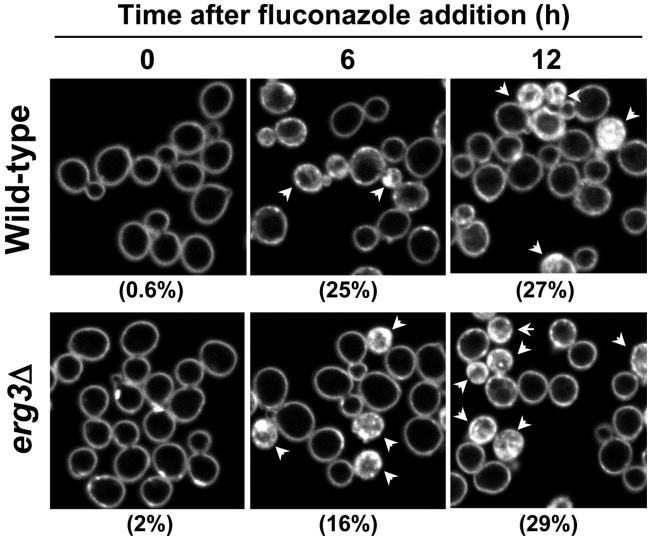

FIGURE 4: Localization of TMA-DPH in cells. Cells of the wild-type strain and the *erg3*Δ mutant were cultured in the presence or absence of 100 μM fluconazole for 6 and 12 h and then labeled with TMA-DPH. The labeled cells were visualized under an FV500 confocal laser microscope. While TMA-DPH was localized solely in the plasma membrane in the absence of fluconazole in both strains, it was distributed throughout the cells in some populations when the cells were incubated with fluconazole. The proportion of abnormally labeled cells was calculated by counting 170−300 cells on fluorescence images.

disordering effect on the isolated plasma membrane (Figure 3B), with S decreasing from 0.965 ± 0.008 (n = 7) to 0.907 ± 0.003 (n = 9) and D_w increasing from 2.0 ± 1.1 μs^{-1} (n = 7) to 9.7 ± 1.2 μs^{-1} (n = 9) (Table 2). However, the degree of those changes appeared to be less marked than in intact cells (Table 1). This apparent difference could be attributable to the incorporation of fluorescence anisotropy signals from TMA-DPH that was distributed throughout the cells in 16−29% of the population (Figure 4). Fluconazole also decreased S in the *erg3*Δ mutant, but S remained at a higher value of 0.922 ± 0.009 (n = 9) (Table 2). Therefore, we assume that C-6 hydroxylation as well as modifications such as C-14 methylation, B-ring saturation, and side-chain alteration acts to decrease membrane order in the wild-type cells after fluconazole treatment. D_w was slightly lower in the *erg3*Δ membrane (8.1 ± 1.2 μs^{-1}, n = 9) than in the wild-type membrane (9.7 ± 1.2 μs^{-1}, n = 9). These results support our hypothesis that 14α-methyl-3,6-diol has less ability to stiffen the lipid bilayer than 14α-methylfecosterol due to the presence of the 6-OH group. The relevance of the S and D_w values to the differential sensitivity to fluconazole in the wild-type strain and the *erg3*Δ mutant is discussed below (see Discussion). Although 10 mM fluconazole markedly inhibits the growth of *erg3*Δ cells (Figure 2A), we did not find any further decrease in S and increase in D_w in the *erg3*Δ plasma membrane compared with the values after 100 μM fluconazole administration (Table 2). This can be explained by the action of fluconazole: even at the lower concentration (100 μM), the drug fully inhibits Erg11 (C-14α-demethylase) regardless of the presence of Erg3. We speculate that 10 mM fluconazole exerts toxicity on the *erg3*Δ cells, possibly due to nonspecific binding to enzymes or partitioning of fluconazole in the membranes, to abolish membrane protein functions.

Measurement of Fluorescence Anisotropy of POPC Membranes. To examine whether the presence of the 6-OH group of sterols generally results in poor membrane packing, we determined the parameters of the POPC membrane containing cholesterol, dihydrocholesterol, or 6α-hydroxy-5α-cholestanol at 30 mol %. The two cholesterol analogues were chosen because they differ from each other by a single chemical feature. Time-resolved anisotropy measurement was carried out at 25 °C, at which the POPC membrane forms a liquid crystalline phase. Figure 5 illustrates the anisotropy decays of TMA-DPH embedded in the artificial membranes along with the structures of the cholesterol derivatives. Consistent with a previous report (*23*), cholesterol highly packed the membrane with a significant increase

Table 2: Effects of Fluconazole on the Anisotropy Decay of TMA-DPH in the Isolated Plasma Membrane of the Wild-Type and *erg3*Δ Cells [a]

fluconazole (mM)	θ (ns)	r_0	r_∞	$S^{b,c}$	D_w (μs^{-1})^{b,c}	$S/D_w{}^{b,c}$	χ^2	n
				Wild-Type Plasma Membrane				
0	7.3 ± 4.6	0.341 ± 0.005	0.317 ± 0.008	0.965 ± 0.008	2.0 ± 1.1	0.60 ± 0.30	1.19 ± 0.10	7
0.1	3.1 ± 0.3	0.340 ± 0.003	0.279 ± 0.003	0.907 ± 0.003**	9.7 ± 1.2**	0.09 ± 0.01**	1.09 ± 0.02	9
10	3.5 ± 0.5	0.342 ± 0.005	0.280 ± 0.006	0.905 ± 0.009**	8.7 ± 1.3**	0.11 ± 0.01**	1.06 ± 0.04	9
				*erg3*Δ Plasma Membrane				
0	3.3 ± 1.8	0.351 ± 0.002	0.331 ± 0.001	0.970 ± 0.004	3.7 ± 1.7	0.34 ± 0.20	1.35 ± 0.31	9
0.1	3.1 ± 0.6	0.346 ± 0.003	0.294 ± 0.008	0.922 ± 0.009**§§	8.1 ± 1.2**§	0.12 ± 0.01**§§	1.24 ± 0.24	9
10	3.1 ± 0.6	0.347 ± 0.003	0.298 ± 0.003	0.927 ± 0.004**§§	7.8 ± 1.8**§	0.12 ± 0.03*	1.23 ± 0.08	8

[a]The plasma membrane was isolated from cells that had been incubated with or without fluconazole for 12 h. Measurements were carried out at 25 °C. Data are represented as mean ± SD. Key: FLC, fluconazole; θ, rotational correlation time; r_0, maximum anisotropy; r_∞, limiting anisotropy; S, order parameter; D_w, rotational diffusion coefficient; n, number of independent experiments. [b]Asterisks denote statistical significance with respect to no fluconazole treatment (*, $P < 0.01$; **, $P < 0.005$). [c]§ denotes statistical significance with respect to the wild-type plasma membrane (§, $P < 0.05$; §§, $P < 0.005$).

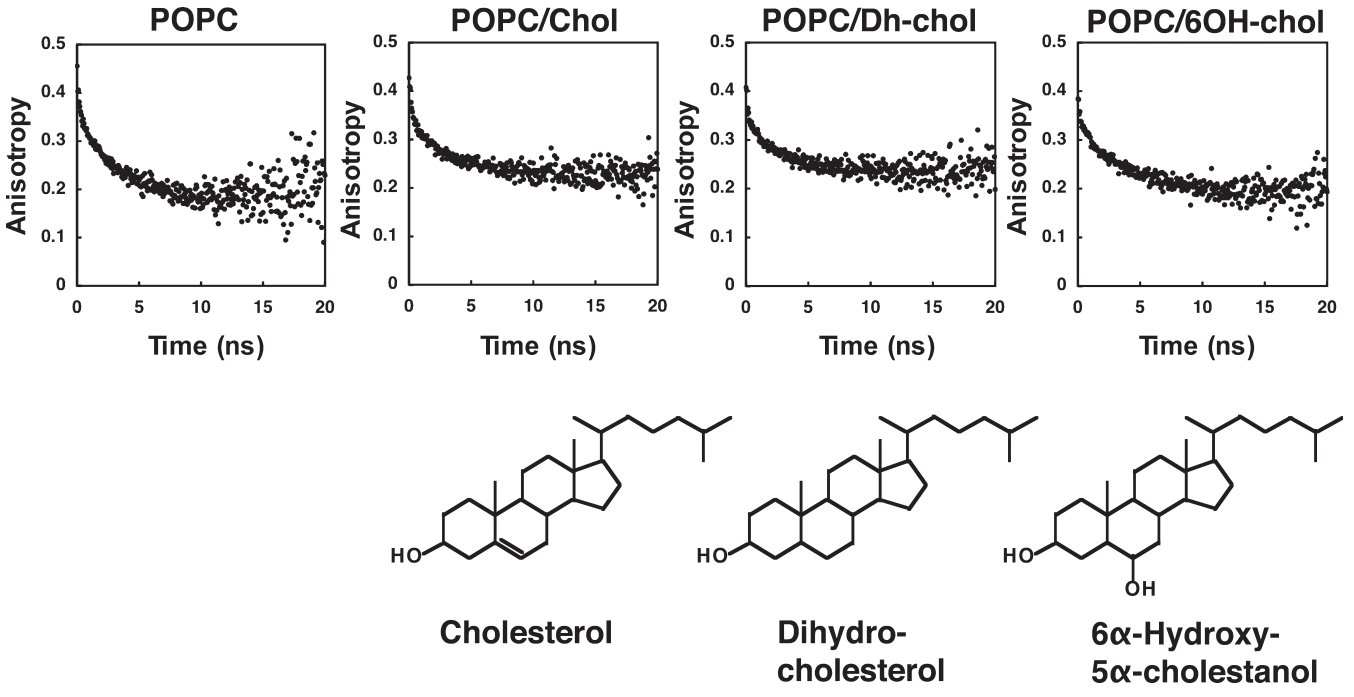

FIGURE 5: Time-resolved anisotropy measurement of TMA-DPH in POPC membranes. Preparation of POPC membranes containing 30 mol % cholesterol (Chol), dihydrocholesterol (Dh-chol), or 6α-hydroxy-5α-cholestanol (6OH-chol) and TMA-DPH is described in the Experimental Procedures. The membranes were subjected to time-resolved anisotropy measurement at 25 °C. The parameters characterizing anisotropy decay are presented in Table 3. The structures of cholesterol, dihydrocholesterol, and 6α-hydroxy-5α-cholestanol are illustrated.

Table 3: Anisotropy Decay of TMA-DPH in POPC Membranes Containing Cholesterol and Its Derivatives[a]

	θ (ns)	r_0	r_∞	S^b	D_w (μs^{-1})^b	$S/D_w{}^b$	χ^2	n
POPC	2.5 ± 0.2	0.335 ± 0.008	0.199 ± 0.007	0.772 ± 0.015	27.1 ± 2.4	0.029 ± 0.003	1.65 ± 0.19	12
POPC/Chol (30 mol %)	2.3 ± 0.2	0.327 ± 0.009	0.236 ± 0.005	0.850 ± 0.009*	20.6 ± 1.9*	0.042 ± 0.004*	1.25 ± 0.08	12
POPC/Dh-chol (30 mol %)	2.3 ± 0.2	0.321 ± 0.009	0.234 ± 0.005	0.854 ± 0.008*	19.6 ± 1.7*	0.044 ± 0.004*	1.26 ± 0.09	12
POPC/6OH-chol (30 mol %)	3.2 ± 0.2	0.327 ± 0.005	0.206 ± 0.010	0.794 ± 0.019*	19.6 ± 1.9*	0.041 ± 0.005*	1.22 ± 0.08	12

[a]Measurements were carried out at 25 °C. Data are represented as mean ± SD. Key: Chol, cholesterol; Dh-chol, dihydrocholesterol; 6OH-chol, 6α-hydroxy-5α-cholestanol; θ, rotational correlation time; r_0, maximum anisotropy; r_∞, limiting anisotropy; S, order parameter; D_w, rotational diffusion coefficient; n, number of independent experiments. [b]Asterisks denote statistical significance with respect to the pure POPC membrane (*, $P < 0.005$).

in S from 0.772 ± 0.015 (n = 12) to 0.850 ± 0.009 (n = 12) (Table 3). The ability to pack the POPC membrane was maintained by dihydrocholesterol that lacks the unsaturated bond in the B-ring (S = 0.854 ± 0.008, n = 12). This is in agreement with a previous report that cholesterol and dihydrocholesterol equally increase the polarization of DPH embedded in the dipalmitoylphosphocholine (DPPC) membrane at 52 °C, at which the membrane forms a liquid crystalline phase (*25*). In contrast, 6-hydroxy-5α-cholestanol marginally increased S of the POPC membrane (=0.794 ± 0.019, n = 12), indicating that the 6-OH

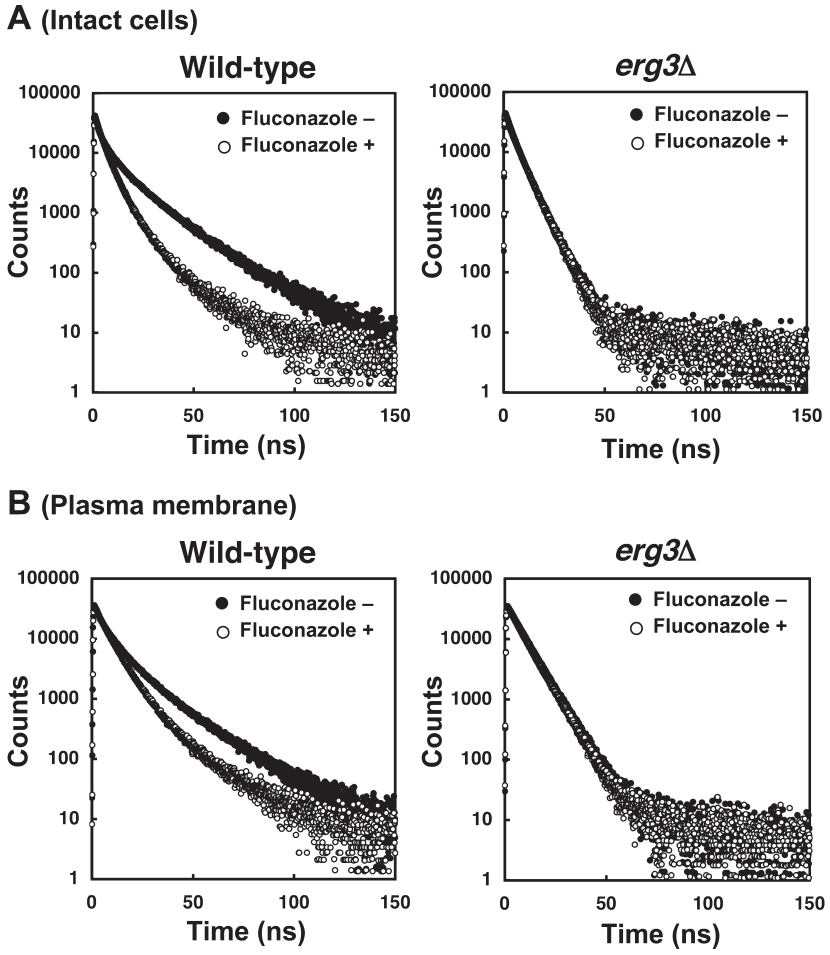

FIGURE 6: Time-resolved lifetime measurement of TMA-DPH in intact cells and plasma membrane isolates. Cells of the wild-type strain and the *erg3*Δ mutant were cultured in the presence or absence of 100 μM fluconazole for 12 h. The cells (A) or the plasma membrane isolated (B) was labeled with 0.5 μM TMA-DPH and subjected to time-resolved anisotropy measurement. The parameters characterizing anisotropy decay are presented in Tables 4 and 5.

group eliminates the ability of sterol to pack the membrane. The finding supports our hypothesis that the 6-OH group of 14α-methyl-3,6-diol interferes with sterol−phospholipid packing of the yeast plasma membrane. Interestingly, the three sterols decreased D_w of the POPC membrane to the same degree from 27.1 μs^{-1} to around 20 μs^{-1}, suggesting that the rotational motion of acyl chains is equally restricted in the presence of these sterols (Table 3). The significance of C-14 methylation is discussed below (see Discussion).

Fluconazole Treatment Allows Water To Penetrate the Plasma Membrane. The fluorescence lifetime depends on the dielectric characteristic of the environment. Because the interfacial region of the membrane is well endowed with proton-accepting groups, such as the carbonyl group of glycerophospholipids and the amide group of sphingolipids, it is natural to assume that molecules with proton-donating groups, such as water and ergosterol, are anchored in the membrane by hydrogen bonding to the interfacial region. Water penetration increases the dielectric constant of the membrane and thereby shortens the fluorescence lifetime of TMA-DPH (*21*, *22*). Figure 6 shows typical fluorescence decays of TMA-DPH in intact cells and the plasma membrane. Lifetime measurement using a model of discrete exponential components allowed observation of the heterogeneity of the wild-type plasma membrane, showing two predominant components of a long lifetime (LLC; τ_1, 18.8 ± 0.1 ns, 50.1 ± 1.9%, n = 10) and a medium one (MLC; τ_2, 6.5 ± 0.2 ns, 40.6 ± 1.8%, n = 10), with a small fraction of a short lifetime component (SLC; τ_3, 1.4 ± 0.1 ns, 9.4 ± 0.8%, n = 10), which is attributable to varying degrees of water penetration into the plasma membrane (Table 4). The heterogeneity of fluorescence lifetime distribution was confirmed in the isolated plasma membrane with LLC (τ_1, 19.8 ± 0.6 ns, 36.2 ± 4.8%, n = 7), MLC (τ_2, 7.5 ± 0.3 ns, 57.9 ± 4.1%, n = 7), and SLC (τ_3, 1.6 ± 0.2 ns, 5.9 ± 0.7%, n = 7) (Table 5). Notably, fluconazole administration eliminated the heterogeneity of the lifetime distribution of TMA-DPH. For example, at 12 h of treatment with 100 μM fluconazole in the isolated plasma membrane, a predominant MLC fraction (τ_2, 7.0 ± 0.2 ns, 82.0 ± 3.2%, n = 9) with a reduced fraction of LLC (τ_1, 18.5 ± 1.3 ns, 10.5 ± 3.5%, n = 9) and SLC (τ_3, 2.2 ± 0.3 ns, 7.4 ± 1.3%, n = 9) was observed (Table 5). Correspondingly, the mean fluorescence lifetime, $\langle\tau\rangle$, decreased from 11.6 ± 0.3 to 7.9 ± 0.2 ns after 100 μM fluconazole treatment. These results suggest that the substitution of 14α-methyl-3,6-diol for ergosterol allowed water molecules to penetrate into the wild-type plasma membrane. Interestingly, we found that deletion of *ERG3* eliminated the heterogeneity of the TMA-DPH lifetime distribution without fluconazole treatment, yielding a predominant MLC fraction (τ_2, 6.1 ± 0.1 ns, 91.7 ± 0.9%, n = 8) and reduced LLC fraction (τ_1, 11.4 ± 0.4 ns, 5.1 ± 1.0%, n = 8) and SLC fraction (τ_3, 1.6 ± 0.3 ns, 3.2 ± 1.0%, n = 8), and $\langle\tau\rangle$ was 6.2 ± 0.1 ns (Table 4). Similar results were obtained in the plasma membrane isolates (Table 5). These results suggest

Table 4: Effects of Fluconazole on the TMA-DPH Lifetime Decay in the Wild-Type and *erg3*Δ Cells[a]

	LLC		MLC		SLC				
time after FLC addition (h)	τ_1 (ns)	A_1 (%)	τ_2 (ns)	A_2 (%)	τ_3 (ns)	A_3 (%)	$\langle\tau\rangle^b$	χ^2	*n*
				Wild-Type Cells					
0	18.8 ± 0.1	50.1 ± 1.9	6.5 ± 0.2	40.6 ± 1.8	1.4 ± 0.1	9.4 ± 0.8	12.2 ± 0.2	1.47 ± 0.10	10
2	18.8 ± 0.4	45.7 ± 2.1	6.6 ± 0.4	44.1 ± 1.4	1.5 ± 0.2	10.2 ± 0.9	11.7 ± 0.2*	1.51 ± 0.14	5
4	16.8 ± 0.5	29.7 ± 1.2	5.7 ± 0.1	58.3 ± 1.8	1.7 ± 0.1	11.9 ± 2.3	8.5 ± 0.1*	1.37 ± 0.04	6
6	14.4 ± 0.1	14.8 ± 0.8	5.0 ± 0.1	74.5 ± 0.3	1.5 ± 0.1	10.7 ± 1.1	6.0 ± 0.1*	1.43 ± 0.12	4
8	14.7 ± 0.3	11.0 ± 0.6	5.1 ± 0.0	77.6 ± 1.1	1.7 ± 0.1	11.4 ± 1.1	5.8 ± 0.0*	1.50 ± 0.06	4
10	14.0 ± 0.7	11.9 ± 0.6	5.2 ± 0.1	77.6 ± 2.1	1.7 ± 0.2	10.6 ± 2.7	5.9 ± 0.1*	1.31 ± 0.06	3
12	15.6 ± 1.4	13.7 ± 1.9	5.4 ± 0.1	75.2 ± 3.0	1.7 ± 0.2	11.1 ± 2.9	6.4 ± 0.4*	1.33 ± 0.11	11
				*erg3*Δ Cells					
0	11.4 ± 0.4	5.1 ± 1.0	6.1 ± 0.1	91.7 ± 0.9	1.6 ± 0.3	3.2 ± 1.0	6.2 ± 0.1	1.35 ± 0.12	8
2	10.7 ± 0.9	7.4 ± 3.6	6.0 ± 0.1	89.0 ± 3.1	1.6 ± 0.2	3.6 ± 1.2	6.1 ± 0.1	1.35 ± 0.08	6
4	11.6 ± 1.0	5.0 ± 2.2	6.1 ± 0.2	91.0 ± 2.1	1.8 ± 0.7	4.2 ± 2.3	6.2 ± 0.1	1.30 ± 0.08	6
6	10.8 ± 1.6	5.4 ± 3.1	5.8 ± 0.1	87.7 ± 2.3	1.9 ± 0.2	6.9 ± 1.5	5.8 ± 0.1*	1.35 ± 0.05	4
8	11.4 ± 1.5	4.1 ± 1.5	5.7 ± 0.2	88.9 ± 0.9	1.8 ± 0.2	7.1 ± 1.0	5.7 ± 0.1*	1.34 ± 0.06	4
10	10.8 ± 0.7	4.2 ± 0.5	5.8 ± 0.2	89.3 ± 3.0	1.8 ± 0.2	6.5 ± 2.6	5.8 ± 0.2*	1.37 ± 0.06	3
12	10.8 ± 1.3	4.4 ± 1.8	5.6 ± 0.2	87.4 ± 1.6	1.8 ± 0.4	8.1 ± 2.4	5.5 ± 0.2*	1.32 ± 0.13	11

[a]Cells were incubated in the presence of 100 μM fluconazole. Measurements were carried out at 25 °C. Data are represented as mean ± SD. Key: LLC, long lifetime component; MLC, medium lifetime component; SLC, short lifetime component; τ, fluorescence lifetime; *A*, amplitude of each fraction; *n*, number of independent experiments. [b]Asterisks denote statistical significance with respect to no fluconazole treatment (*, $P < 0.005$).

Table 5: Effects of Fluconazole on the TMA-DPH Lifetime Decay in the Isolated Plasma Membrane of the Wild-Type and *erg3*Δ Cells[a]

	LLC		MLC		SLC				
fluconazole	τ_1 (ns)	A_1 (%)	τ_2 (ns)	A_2 (%)	τ_3 (ns)	A_3 (%)	$\langle\tau\rangle^{b,c}$	χ^2	*n*
				Wild-Type Plasma Membrane					
0	19.8 ± 0.6	36.2 ± 4.8	7.5 ± 0.3	57.9 ± 4.1	1.6 ± 0.2	5.9 ± 0.7	11.6 ± 0.3	1.39 ± 0.12	7
0.1	18.5 ± 1.3	10.5 ± 3.5	7.0 ± 0.2	82.0 ± 3.2	2.2 ± 0.3	7.4 ± 1.3	7.9 ± 0.2*	1.32 ± 0.08	9
10	16.9 ± 1.6	10.0 ± 1.8	6.9 ± 0.2	83.5 ± 1.2	2.1 ± 0.3	6.5 ± 1.5	7.6 ± 0.1*	1.29 ± 0.09	9
				*erg3*Δ Plasma Membrane					
0	15.0 ± 3.9	5.0 ± 2.1	7.5 ± 0.1	94.2 ± 2.1	1.2 ± 0.0	0.8 ± 0.1	7.7 ± 0.1	1.26 ± 0.10	9
0.1	15.2 ± 3.9	4.4 ± 2.8	7.1 ± 0.1	92.7 ± 2.3	1.9 ± 0.6	2.8 ± 1.2	7.2 ± 0.1*§	1.28 ± 0.09	9
10	17.6 ± 9.1	4.1 ± 3.4	7.2 ± 0.2	92.4 ± 3.3	1.9 ± 1.0	3.5 ± 3.0	7.3 ± 0.1*§	1.26 ± 0.10	8

[a]The plasma membrane was isolated from cells that had been incubated with or without fluconazole for 12 h. Measurements were carried out at 25 °C. Data are represented as mean ± SD. Key: LLC, long lifetime component; MLC, medium lifetime component; SLC, short lifetime component; τ, fluorescence lifetime; *A*, amplitude of each fraction; *n*, number of independent experiments. [b]Asterisks denote statistical significance with respect to no fluconazole treatment (*, $P < 0.005$). [c]§ denotes statistical significance with respect to the wild-type plasma membrane (§, $P < 0.005$).

that the *erg3*Δ plasma membrane allowed water penetration, leading to membrane homogeneity with respect to the dielectric characteristic. Fluconazole treatment did not appreciably influence the TMA-DPH lifetime in *erg3*Δ cells (Tables 4 and 5). We did not find any further changes in the fluorescence lifetime and its distribution when cells were exposed to a higher concentration of 10 mM fluconazole. Therefore, we conclude that specific structural motifs of ergosterol are required to prevent water penetration into the plasma membrane. Our findings can be accommodated by the schematic diagram depicted in Figure 7.

DISCUSSION

Comparison of the plasma membrane properties between the wild-type strain and the *erg3*Δ mutant makes it possible to identify the features of the 14α-methyl-3,6-diol molecule critical for the deleterious impact of fluconazole on membrane packing and viability of the cells. Judging from the changes in the order parameter *S* and the rotational diffusion coefficient D_w with or without fluconazole treatment, the presence of the 6-OH group appears not to be the sole factor accounting for the fluconazole-induced membrane disorder, and the occurrence of C-14 methylation, B-ring saturation, and/or side-chain modification act additively to decrease membrane rigidity (Table 2). In artificial membranes, the double bonds in the B-ring have been suggested to increase the interactions with phospholipid acyl chains due to van der Waals forces, increasing the planarity of the ring (*26*). A molecular dynamic simulation study indicated that ergosterol has a higher condensing effect on the membrane, as reflected by the area per lipid, and ergosterol also positions itself close to the bilayer−water interface (*27*). Lanosterol has three additional

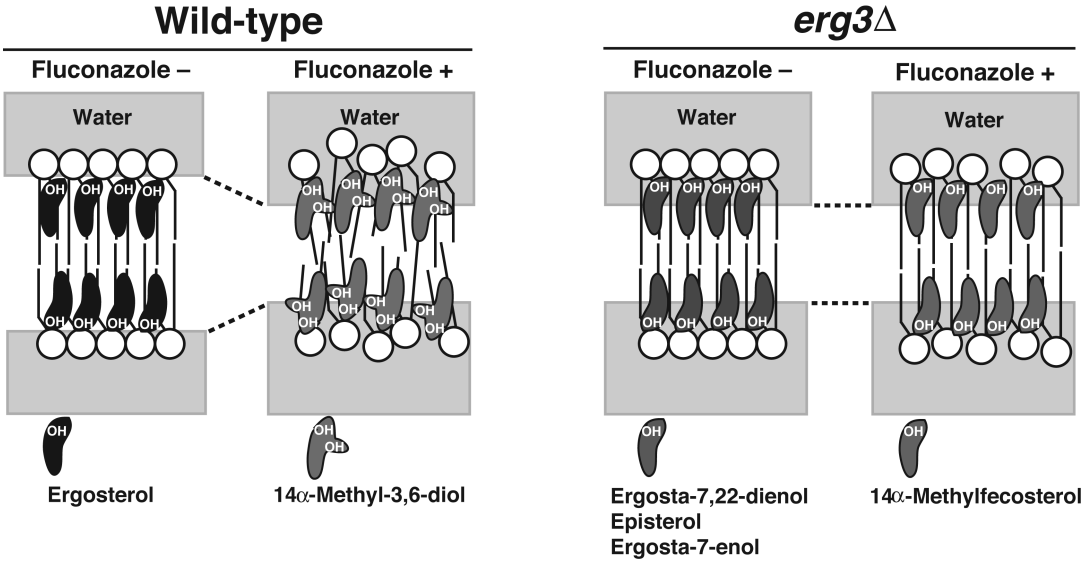

FIGURE 7: Schematic diagram of changes in plasma membrane properties associated with sterol modifications after fluconazole administration.

methyl groups compared with cholesterol and ergosterol, two of which are attached to C-4 and the third attached to C-14 as seen in 14α-methyl-3,6-diol and 14α-methylfecosterol, and therefore lanosterol is bulkier than cholesterol and ergosterol. Lanosterol also locates relatively more centrally in the bilayer, and consequently it orders and packs the lipid acyl chains less well than the others (*27*). The behavior of cholesterol is intermediate between ergosterol and lanosterol. Therefore, it is natural to assume that 14α-methylfecosterol and further 14α-methyl-3,6-diol have poor membrane packing abilities compared with ergosterol, and this could account for the significant decrease in S after fluconazole administration in both strains. It is possible that the presence of the 6-OH group of 14α-methyl-3,6-diol results in a decreasing order parameter in the wild-type strain ($S = 0.907 \pm 0.003$) compared with that in the *erg3*Δ mutant ($S = 0.922 \pm 0.009$). These findings agree well with our results of fluorescence lifetime measurement showing that water penetration into the plasma membrane is enhanced after fluconazole treatment, reflected by the shortening of the average fluorescence lifetime, $\langle\tau\rangle$, of TMA-DPH in the wild-type plasma membrane (Table 5). This is consistent with previous studies showing that cholesterol and ergosterol prevent water penetration into artificial membranes, reflected by the lengthening $\langle\tau\rangle$ of TMA-DPH (*28*). However, the changes in S and D_w determined in our study did not fully correspond to the observed decrease in $\langle\tau\rangle$. Specifically, deletion of *ERG3* allowed water penetration without fluconazole treatment, as observed in the wild-type strain with fluconazole treatment (Table 5) although S remained high (Table 2). Parks and colleagues showed that an ergosterol auxotrophic mutant alters the fatty acid composition of lipids by an increase in unsaturated fatty acids such as palmitoleic and oleic acid and a concomitant decrease in palmitic acid when the growth is supported by cholesterol or cholestanol (dihydrocholesterol) (*29*). The *erg3*Δ cells accumulate altered sterols, such as ergosta-7, 22-dienol, and episterol and ergosta-7-enol in the plasma membrane (ref *30* and Figure 1). Accordingly, it is possible that the *erg3*Δ cells alter the fatty acid composition of the plasma membrane in response to the accumulation of structurally different sterols. Particularly, the sterol−lipid interactions might be weakened by the compositional alteration, allowing water penetration without affecting the order parameter. A recent report has shown that cells adjust the membrane composition in response to *erg* mutations by preferentially changing the sphingolipid composition (*31*). Further experiments are necessary to validate the link between the lipid/sterol composition, membrane rigidity, and degree of water penetration.

How the changes in membrane rigidity account for the differential sensitivity to fluconazole of the wild-type strain and *erg3*Δ mutant remains unresolved. There could be a critical point in the membrane order parameter between 0.907 and 0.922, which separates the growth of the wild-type and *erg3*Δ cells. Nes et al. reported the structural requirements of sterols to support the growth of an ergosterol auxotrophic mutant. They concluded that the ring double bonds and the presence or absence of the C-14 methyl group were nonessential, but the 3β-OH group and the longest methylene segment extending from C-20 but not exceeding six contiguous C-atoms were essential to support mutant growth, although the C-14 methyl group was not examined (*32*). It would be worthwhile to determine the membrane properties in the ergosterol auxotrophic mutant in which growth is supported by various sterols and their derivatives. It is also likely that the polar 6-OH group of 14α-methyl-3,6-diol has a deleterious impact on lipid−protein interactions or membrane protein activities due to unfavorable hydrogen bonding and/or steric hindrance. The activities of a number of membrane proteins are known to be modulated by the physical state of the membrane lipids with respect to acyl chain unsaturation, the presence of sterols, or hydration (*33*). The conformation of integral membrane proteins can be affected by changes in the dielectric constant due to changes in electric miltipole−multipole interactions (*34*, *35*). Accordingly, fluconazole treatment is likely to diminish the functions of some yeast plasma membrane proteins. Furthermore, membrane-associated cellular processes such as endocytosis, vesicle fusion, or membrane trafficking could be affected by the presence of the 6-OH group. According to genome-wide transcriptional analysis, fluconazole upregulates a number of genes including nine ergosterol-biosynthetic genes (*36*). Such a remodeling of cellular components renders an intricate outcome that affects the phenotypic trait of the cells upon fluconazole administration.

Our results of fluorescence lifetime measurement using a model of discrete exponential components allowed observation

of the heterogeneity of the wild-type plasma membrane in terms of the dielectric characteristic, most probably corresponding to the variation in water penetration. Such membrane heterogeneity was also observed in rat hepatocytes and liver (*37*) and human granulocytes (*38*) using TMA-DPH fluorescence lifetime analysis. The mathematical basis for the distributional approach agrees with the raft concept commonly evaluated using the detergent solubility assay (*39*). Ergosterol has more pronounced effects on domain formation in the sphingolipid/DPPC membrane than cholesterol (*40*). Macroscopic segregation of Pma1 and the arginine permease Can1 was observed in the plasma membrane (*41*). However, it is unclear whether the membrane heterogeneity demonstrated in this study corresponds to the lateral segregation of these membrane proteins. We assume that experiments with fluconazole on *S. cerevisiae* cells could confirm the relevance of lateral segregation of lipid molecules and membrane proteins and the association of the proteins with detergent-resistant membranes.

ACKNOWLEDGMENT

We thank Koki Horikoshi, Shoji Kaneshina, Hitoshi Matsuki, Roland Winter, Jun Kawamoto, and Satoshi B. Sato for helpful discussions.

REFERENCES

1. Ben-Ami, R., Lewis, R. E., and Kontoyiannis, D. P. (2008) Immunocompromised hosts: immunopharmacology of modern antifungals. *Clin. Infect. Dis. 47*, 226–235.
2. Kanafani, Z. A., and Perfect, J. R. (2008) Antimicrobial resistance: resistance to antifungal agents: mechanisms and clinical impact. *Clin. Infect. Dis. 46*, 120–128.
3. Kalb, V. F., Woods, C. W., Turi, T. G., Dey, C. R., Sutter, T. R., and Loper, J. C. (1987) Primary structure of the P450 lanosterol demethylase gene from *Saccharomyces cerevisiae*. *DNA 6*, 529–537.
4. Lupetti, A., Danesi, R., Campa, M., Del Tacca, M., and Kelly, S. (2002) Molecular basis of resistance to azole antifungals. *Trends Mol. Med. 8*, 76–81.
5. Morschhauser, J. (2002) The genetic basis of fluconazole resistance development in *Candida albicans*. *Biochim. Biophys. Acta 1587*, 240–248.
6. Watson, P. F., Rose, M. E., Ellis, S. W., England, H., and Kelly, S. L. (1989) Defective sterol C5-6 desaturation and azole resistance: a new hypothesis for the mode of action of azole antifungals. *Biochem. Biophys. Res. Commun. 164*, 1170–1175.
7. Kelly, S. L., Lamb, D. C., Corran, A. J., Baldwin, B. C., and Kelly, D. E. (1995) Mode of action and resistance to azole antifungals associated with the formation of 14α-methylergosta-8,24(28)-dien-3β, 6α-diol. *Biochem. Biophys. Res. Commun. 207*, 910–915.
8. Kinosita, K., Jr., Kawato, S., and Ikegami, A. (1977) A theory of fluorescence polarization decay in membranes. *Biophys. J. 20*, 289–305.
9. Prendergast, F. G., Haugland, R. P., and Callahan, P. J. (1981) 1-[4-(Trimethylamino)phenyl]-6-phenylhexa-1,3,5-triene: synthesis, fluorescence properties, and use as a fluorescence probe of lipid bilayers. *Biochemistry. 20*, 7333–7338.
10. Lentz, B. R. (1993) Use of fluorescent probes to monitor molecular order and motions within liposome bilayers. *Chem. Phys. Lipids 64*, 99–116.
11. van Langen, H., van Ginkel, G., Shaw, D., and Levine, Y. K. (1989) The fidelity of response by 1-[4-(trimethylammonio)phenyl]-6-phenyl-1,3,5-hexatriene in time-resolved fluorescence anisotropy measurements on lipid vesicles. Effects of unsaturation, headgroup and cholesterol on orientational order and reorientational dynamics. *Eur. Biophys. J. 17*, 37–48.
12. Low, C., Rodriguez, R. J., and Parks, L. W. (1985) Modulation of yeast plasma membrane composition of a yeast sterol auxotroph as a function of exogenous sterol. *Arch. Biochem. Biophys. 240*, 530–538.
13. Vogel, J. P., Lee, J. N., Kirsch, D. R., Rose, M. D., and Sztul, E. S. (1993) Brefeldin A causes a defect in secretion in *Saccharomyces cerevisiae*. *J. Biol. Chem. 268*, 3040–3043.
14. Inoue, T., Iefuji, H., Fujii, T., Soga, H., and Satoh, K. (2000) Cloning and characterization of a gene complementing the mutation of an ethanol-sensitive mutant of sake yeast. *Biosci. Biotechnol. Biochem. 64*, 229–236.
15. Emter, R., Heese-Peck, A., and Kralli, A. (2002) *ERG6* and *PDR5* regulate small lipophilic drug accumulation in yeast cells via distinct mechanisms. *FEBS Lett. 521*, 57–61.
16. Mukhopadhyay, K., Kohli, A., and Prasad, R. (2002) Drug susceptibilities of yeast cells are affected by membrane lipid composition. *Antimicrob. Agents Chemother. 46*, 3695–3705.
17. Abe, F., and Hiraki, T. (2009) Mechanistic role of ergosterol in membrane rigidity and cycloheximide resistance in *Saccharomyces cerevisiae*. *Biochim. Biophys. Acta 1788*, 743–752.
18. Abe, F., and Minegishi, H. (2008) Global screening of genes essential for growth in high-pressure and cold environments: searching for basic adaptive strategies using a yeast deletion library. *Genetics 178*, 851–872.
19. Giaever, G., Chu, A. M., Ni, L., Connelly, C., Riles, L., Veronneau, S., Dow, S., Lucau-Danila, A., Anderson, K., Andre, B., Arkin, A. P., Astromoff, A., El-Bakkoury, M., Bangham, R., Benito, R., Brachat, S., Campanaro, S., Curtiss, M., Davis, K., Deutschbauer, A., Entian, K. D., Flaherty, P., Foury, F., Garfinkel, D. J., Gerstein, M., Gotte, D., Guldener, U., Hegemann, J. H., Hempel, S., Herman, Z., Jaramillo, D. F., Kelly, D. E., Kelly, S. L., Kotter, P., LaBonte, D., Lamb, D. C., Lan, N., Liang, H., Liao, H., Liu, L., Luo, C., Lussier, M., Mao, R., Menard, P., Ooi, S. L., Revuelta, J. L., Roberts, C. J., Rose, M., Ross-Macdonald, P., Scherens, B., Schimmack, G., Shafer, B., Shoemaker, D. D., Sookhai-Mahadeo, S., Storms, R. K., Strathern, J. N., Valle, G., Voet, M., Volckaert, G., Wang, C. Y., Ward, T. R., Wilhelmy, J., Winzeler, E. A., Yang, Y., Yen, G., Youngman, E., Yu, K., Bussey, H., Boeke, J. D., Snyder, M., Philippsen, P., Davis, R. W., and Johnston, M. (2002) Functional profiling of the *Saccharomyces cerevisiae* genome. *Nature 418*, 387–391.
20. Abe, F., and Iida, H. (2003) Pressure-induced differential regulation of the two tryptophan permeases Tat1 and Tat2 by ubiquitin ligase Rsp5 and its binding proteins, Bul1 and Bul2. *Mol. Cell. Biol. 23*, 7566–7584.
21. Ho, C., Slater, S. J., and Stubbs, C. D. (1995) Hydration and order in lipid bilayers. *Biochemistry 34*, 6188–6195.
22. Bernsdorff, C., Wolf, A., Winter, R., and Gratton, E. (1997) Effect of hydrostatic pressure on water penetration and rotational dynamics in phospholipid-cholesterol bilayers. *Biophys. J. 72*, 1264–1277.
23. Sutter, M., Fiechter, T., and Imanidis, G. (2004) Correlation of membrane order and dynamics derived from time-resolved fluorescence measurements with solute permeability. *J. Pharm. Sci. 93*, 2090–2107.
24. Anderson, J. B., Sirjusingh, C., Parsons, A. B., Boone, C., Wickens, C., Cowen, L. E., and Kohn, L. M. (2003) Mode of selection and experimental evolution of antifungal drug resistance in *Saccharomyces cerevisiae*. *Genetics 163*, 1287–1298.
25. Xu, X., and London, E. (2000) The effect of sterol structure on membrane lipid domains reveals how cholesterol can induce lipid domain formation. *Biochemistry 39*, 843–849.
26. Urbina, J. A., Pekerar, S., Le, H. B., Patterson, J., Montez, B., and Oldfield, E. (1995) Molecular order and dynamics of phosphatidylcholine bilayer membranes in the presence of cholesterol, ergosterol and lanosterol: a comparative study using ^{2}H-, ^{13}C- and ^{31}P-NMR spectroscopy. *Biochim. Biophys. Acta 1238*, 163–176.
27. Cournia, Z., Ullmann, G. M., and Smith, J. C. (2007) Differential effects of cholesterol, ergosterol and lanosterol on a dipalmitoyl phosphatidylcholine membrane: a molecular dynamics simulation study. *J. Phys. Chem. B 111*, 1786–1801.
28. Konopasek, I., Kvasnicka, P., Amler, E., Kotyk, A., and Curatola, G. (1995) The transmembrane gradient of the dielectric constant influences the DPH lifetime distribution. *FEBS Lett. 374*, 338–340.
29. Bottema, C. D., Rodriguez, R. J., and Parks, L. W. (1985) Influence of sterol structure on yeast plasma membrane properties. *Biochim. Biophys. Acta 813*, 313–320.
30. Heese-Peck, A., Pichler, H., Zanolari, B., Watanabe, R., Daum, G., and Riezman, H. (2002) Multiple functions of sterols in yeast endocytosis. *Mol. Biol. Cell 13*, 2664–2680.
31. Guan, X. L., Souza, C. M., Pichler, H., Dewhurst, G., Schaad, O., Kajiwara, K., Wakabayashi, H., Ivanova, T., Castillon, G. A., Piccolis, M., Abe, F., Loewith, R., Funato, K., Wenk, M. R., and Riezman, H. (2009) Functional interactions between sphingolipids and sterols in biological membranes regulating cell physiology. *Mol. Biol. Cell 20*, 2083–2095.
32. Nes, W. D., Janssen, G. G., Crumley, F. G., Kalinowska, M., and Akihisa, T. (1993) The structural requirements of sterols for membrane

function in *Saccharomyces cerevisiae*. *Arch. Biochem. Biophys. 300*, 724–733.
33. Sotomayor, C. P., Aguilar, L. F., Cuevas, F. J., Helms, M. K., and Jameson, D. M. (2000) Modulation of pig kidney Na^+/K^+-ATPase activity by cholesterol: role of hydration. *Biochemistry 39*, 10928–10935.
34. Teissie, J. (2007) Biophysical effects of electric fields on membrane water interfaces: a mini review. *Eur. Biophys. J. 36*, 967–972.
35. Disalvo, E. A., Lairion, F., Martini, F., Tymczyszyn, E., Frias, M., Almaleck, H., and Gordillo, G. J. (2008) Structural and functional properties of hydration and confined water in membrane interfaces. *Biochim. Biophys. Acta 1778*, 2655–2670.
36. Bammert, G. F., and Fostel, J. M. (2000) Genome-wide expression patterns in *Saccharomyces cerevisiae*: comparison of drug treatments and genetic alterations affecting biosynthesis of ergosterol. *Antimicrob. Agents Chemother. 44*, 1255–1265.
37. Ferretti, G., Zolese, G., Curatola, G., Jezequel, A. M., and Benedetti, A. (1993) Membrane heterogeneity in isolated rat hepatocytes and liver plasma membrane subfractions: a comparative study using DPH and its cationic derivative TMA-DPH. *Biochim. Biophys. Acta 1147*, 245–250.
38. Valentino, M., Governa, M., Gratton, E., Fiorini, R., Curatola, G., and Bertoli, E. (1988) Increased membrane heterogeneity in stimulated human granulocytes. *FEBS Lett. 234*, 451–454.
39. Bagnat, M., Chang, A., and Simons, K. (2001) Plasma membrane proton ATPase Pma1p requires raft association for surface delivery in yeast. *Mol. Biol. Cell 12*, 4129–4138.
40. Xu, X., Bittman, R., Duportail, G., Heissler, D., Vilcheze, C., and London, E. (2001) Effect of the structure of natural sterols and sphingolipids on the formation of ordered sphingolipid/sterol domains (rafts). Comparison of cholesterol to plant, fungal, and disease-associated sterols and comparison of sphingomyelin, cerebrosides, and ceramide. *J. Biol. Chem. 276*, 33540–33546.
41. Malinska, K., Malinsky, J., Opekarova, M., and Tanner, W. (2003) Visualization of protein compartmentation within the plasma membrane of living yeast cells. *Mol. Biol. Cell 14*, 4427–4436.